ARTICLE

First principles and experimental studies of empty Si_{46} as anode materials for Li-ion batteries

Kwai S. Chan,[a] Michael A. Miller, Wuwei Liang, and Carol Ellis-Terrell
Department of Materials Engineering, Mechanical Engineering Division, Southwest Research Institute®, San Antonio, TX 78238-5166, USA

Candace K. Chan
Materials Science and Engineering, School for Engineering of Matter, Transport and Energy, Arizona State University, Tempe, AZ 85287-8706, USA

(Received 12 July 2016; accepted 19 October 2016)

The objective of this investigation was to utilize the first-principles molecular dynamics computational approach to investigate the lithiation characteristics of empty silicon clathrates (Si_{46}) for applications as potential anode materials in lithium-ion batteries. The energy of formation, volume expansion, and theoretical capacity were computed for empty silicon clathrates as a function of Li. The theoretical results were compared against experimental data of long-term cyclic tests performed on half-cells using electrodes fabricated from Si_{46} prepared using a Hofmann-type elimination–oxidation reaction. The comparison revealed that the theoretically predicted capacity (of 791.6 mAh/g) agreed with experimental data (809 mAh/g) that occurred after insertion of 48 Li atoms. The calculations showed that overlithiation beyond 66 Li atoms can cause large volume expansion with a volume strain as high as 120%, which may correlate to experimental observations of decreasing capacities from the maximum at 1030 mAh/g to 553 mA h/g during long-term cycling tests. The finding suggests that overlithiation beyond 66 Li atoms may have caused damage to the cage structure and led to lower reversible capacities.

I. INTRODUCTION

Silicon is an attractive anode material for Li-ion batteries because its theoretical charge storage capacity (3579 mAh/g as $Li_{15}Si_4$) is more than 10 times than that of graphite,[1] the current anode material in commercial cells. Despite a high theoretical charge capacity, silicon has not been successfully utilized as the anode in Li-ion batteries because the reversible reaction of lithium with silicon is accompanied by large (~300%) changes in volume. The large increase in volume, which is isotropic in amorphous Si, can cause Si particles to displace and impinge on other parts of the anode.[2] Such particle motion has been directly observed using in situ atomic force[3] and optical microscopes.[4] Theoretical studies on electrodes made of Si particles have found that in order for the particles to be adequately spaced to avoid displacement, they must occupy only 20 vol% of the electrode, whereas the remaining mass consists of the binder and conducting additives.[5] This composition leads to a serious reduction in energy density because the active Si material makes up only a small percentage of the electrode.

Furthermore, the large volume mismatch between the unlithiated and lithiated phases often results in large internal stresses[6] that cause the Si to delaminate from the electrode (decrepitation) or form smaller particles (pulverization) that are detached from the current collector. Mixing or ball-milling the Si with binders or other networking agents (such as carbon nanotubes[7–9]) have not completely solved these problems, as the volume changes are too large for adequate binding. Upon delithiation, Si-based electrodes will display features characterized by shrinkage due to the removal of large amounts of lithium. For instance, micropillars can shrink in size,[3] and thin films can form cracks. Extensive shrinkage or pulverization often causes the anode to lose electronic or mechanical contact with the current collector. The consequences are loss of active material, poor discharge/charge efficiencies (coulombic efficiency), and reduced capacity over time. For example, as much as 85% capacity loss was observed after only 5 cycles in electrodes made with 10 μm Si particles.[10]

To solve the decrepitation problem, several electrode morphologies and architectures have been explored to relax the strain and allow the volume changes without subsequent pulverization.[11] Promising results have been demonstrated by using nanostructured thin films,[12,13] particles,[12] porous structures,[14] pillars,[15] nanowires,[16,17]

Contributing Editor: Chongmin Wang
[a]Address all correspondence to this author.
e-mail: kchan@swri.edu
DOI: 10.1557/jmr.2016.408

or double-walled silicon-nanotubes.[18,19] All of these structures have been designed to allow room for volume expansion and relaxation of the triaxial tensile stresses. Long-term cycling (>100 cycles) at capacities close to the theoretical capacity of Si have yet to be demonstrated because the problem associated with the large volume change has not been completely resolved, although progress has been made on several fronts.[18,19] By constraining the outer wall and directing the volume of expansion inward, long-term cycling of double-walled silicon nanotube electrodes in the range of 600–1000 mAh/g has been demonstrated for 6000 cycles.[18,19]

Recent studies have focused on the use of ab initio methods to evaluate the performance of electrode materials,[20] including simulating the Li insertion and de-insertion processes in crystalline Si,[21,22] amorphous Si,[23,24] and Si nanowires.[25] In particular, ab initio methods have been utilized to compute the energy of formation,[21–24] the electronic structure,[21,23,24] the open-circuit potential,[20–24] the volume change,[22] and the diffusion path[25] of the lithiated phases. Despite these efforts, the problems associated with the volume shrinkage and pulverization during delithiation have not been resolved.

Besides conventional crystalline Si (diamond cubic) and amorphous Si, other allotropes of Si such as silicon clathrates (Type I, II, or III) may also be lithiated. Silicon clathrates consist of sp^3 bonded silicon atoms arranged in one of three types (Type I, II, and III) of cage-structures.[29,30] Type I silicon clathrate Si_{46}, which consists of Si with a regular arrangement of 20-atom and 24-atom cages fused together through 5-atom pentagonal rings, has a simple cubic structure with a lattice parameter of 10.335 Å and 46 Si atoms per unit cell.[29] The crystal structure (space group $Pm\bar{3}n$) of the Si_{46} clathrate is different from the common form of crystalline Si (c-Si), which is diamond cubic (space group $Fd\bar{3}m$) with a lattice parameter of about 5.456 Å.[31] Another form of silicon clathrate (Type II) is Si_{34} that contains Si with a regular arrangement of 20-atom and 28-atom cages fused together through 5-atom pentagonal rings. The Si_{34} clathrate has a face-centered cubic (fcc) structure, with 136 Si atoms per fcc unit cell.[29] The Si_{34} clathrate has a lattice parameter of 14.62 Å and belongs to the space group $Fd\bar{3}m$, number 227. Type III clathrates can be considered a variant of Type I clathrates with a different ratio of 20-atom and 24-atom cages.[30] Recent work by the authors identified empty Si_{46} and Ba-stabilized Al-substituted clathrates as potential Type I clathrate anode materials for Li-ion batteries.[26] Lithiation of Ba-stabilized Al-substituted clathrates has been confirmed by recent experimental and theoretical investigations.[26–28] Lithiation of empty Si_{46}, however, has not been reported because synthesis of empty Si_{46} is difficult. Thus, the lithiation response of empty Si_{46} has not been established either theoretically or experimentally.

In this paper, we examine the lithiation characteristics of empty silicon clathrate (Si_{46}) via first-principles molecular dynamics computational methods. The energy of formation and the equilibrium lattice constant of Li_xSi_{46} are computed as a function of number of Li atoms inserted into the cage structure. The theoretical capacities and volume expansion of the unit cell associated with the lithiation were examined as a function of Li atoms ranging from 1 to 200. The theoretical results indicate that up to 23–24 Li can be inserted into empty Si_{46} without volume expansion (less than 2.3% volume strain). Both the capacities and calculated volume expansion increase with further lithiation, reaching a capacity of 809 and 1030 mAh/g at 48 and 66 Li atoms inserted, respectively. Motivated by the theoretical results, we have developed a solution synthesis method that successfully produced small quantities of empty Si_{46}. Furthermore, empty Si_{46} electrodes were fabricated to characterize their response to lithiation. The theoretical lithiation response was compared against the experimental observations to assess the potential of empty Si_{46} as an anode material in Li-ion batteries.

II. METHODS

A. Computational details

First-principles methods have been utilized to model lithiation characteristics for many Li-ion battery materials.[20–25] The energy calculations were performed using an ab initio molecular dynamics code, the Car–Parrinello molecular dynamics (CPMD) code,[32] which is a plane wave implementation of density functional theory (DFT).[33] It uses an approximation frozen-core approach in which only the chemically active valence electrons are explicitly dealt with and the inert core electrons are considered frozen together with the nuclei as rigid non-polarizable ion cores. It is capable of both first principles wave-function optimization (static calculation) and ab initio molecular dynamics calculations. For crystalline solids, the energy and equilibrium lattice constant of a unit cell were computed by calculating the energies for unit cells with different lattice constants by performing wave-function optimization with CPMD. A 4th-order polynomial was fitted to the energy points. The equilibrium lattice constant was determined by finding the lattice constant corresponding to the minimum energy on the polynomial curve. The energy of an amorphous phase was computed by heating the corresponding crystalline phase above the melting point, followed by rapid quenching to 300 K and holding at this temperature as a function of time to allow for atom relaxation and equilibrium to occur. Using the CPMD method,[32,33] first principles computations were performed to determine the energy of formation for

crystalline Si (c-Si), amorphous Si (a-Si), crystalline $Li_{15}Si_4$ (c-$Li_{15}Si_4$), crystalline Si_{46} clathrate (c-Si_{46}), and Type I crystalline lithium–silicon clathrates (c-Li_xSi_{46}) with x ranging from 1 to 200. For $x < 8$ Li atoms, the Li atoms were placed at the 8 known sites (2a and 6d) corresponding to the centers of the cavities within the cages. For lithiation in excess of 8 Li atoms, the Li atoms were placed randomly within the cage structure and the Li atoms were allowed to move to their equilibrium locations during energy optimization.

B. Experimental details

Empty Si_{46} was synthesized in a batch process which involved soft oxidation of Na_4Si_4 by a Hofmann-type elimination–oxidation reaction scheme.[34] First, a thermal processing method was devised to convert commercial fuel-grade sodium silicide ($NaSi_{1.5}$) to yield the highest purity of the Zintl phase Na_4Si_4 possible by varying excess additions of NaH combined with the silicide. X-ray diffraction (XRD) analyses of the thermal transformation products confirmed the conversion of $NaSi_{1.5}$ to the Zintl phase Na_4Si_4, when 10% excess NaH was combined with the silicide during thermal processing. Higher additions of NaH did not manifest the required XRD reflections for the Zintl phase. Using these processing conditions, about 10 g of Na_4Si_4 was synthesized for subsequent use in the batch synthesis of Si_{46}. After successful conversion of Na_4Si_4, this Zintl compound was combined with an alkylammonium-$AlCl_3$ ionic liquid to synthesize empty silicon clathrate (Si_{46}) via Hofmann-type elimination–oxidation reaction scheme done in solution.[34,35] The XRD analysis of the reaction product indicated that the desired Type I clathrate was formed along with unreacted Zintl compound and the reaction by-products. The reaction by-products were expected to be alkene, alkylamines, and Na_4Si_9. Energy dispersive X-ray spectroscopy indicated that the amount of Si_{46} formed was about 18.1% by weight. The product (~20 mg) was cleaned with copious amounts of acetone to remove the organic by-products (alkene and alkylamines) and any ionic liquid. The cleaning process did not completely remove all of the reaction by-products as some extra peaks still remained in the XRD pattern, as shown in Fig. 1. Attempts to further purify the products caused a loss of Si_{46}. Thus, further purification of the Si_{46} products was abandoned and the Si_{46} products were used for half-cell testing after acetone-cleaned conditions.

Guest-free (empty) Si_{46} clathrates synthesized by soft oxidation of Na_4Si_4 were combined with a conducting carbon black additive (25 wt% Super P) and polyvinylidene difluoride binder (20 wt%) to make a slurry. The resulting slurries were then used to cast thin-film electrodes for electrochemical half-cell evaluation. The long-term cyclic performance of guest-free Si_{46} was evaluated using a three-electrode split cell with a polypropylene separator film and Li metal counter and reference electrodes. The active area of the electrode was also 1.766 cm^2 with a thickness of 89.2 μm. The mass of the active material was 0.3485 mg. The electrolyte was 1 M $LiPF_6$ in ethylene carbonate (EC)/diethyl carbonate (DEC)/ fluroethylene carbonate (FEC) in 45:45:10 volume ratios. The half-cell testing was conducted according to a galvanostatic cycling protocol described as follows. The targeted voltage was cycled between 1 V and 5 mV versus Li/Li^+ for cycles 1 to 3 at a C rate of C/5 for the solid electrolyte interphase (SEI) formation phase. After SEI formation, the voltage cycling range was maintained from 1 V to 5 mV versus Li/Li^+ but the C rate was increased to 5.3 for the rest of the long-term cyclic tests until the tests were terminated after 1000 cycles. The C rates were computed on the basis of the mass of the active materials in the electrode.

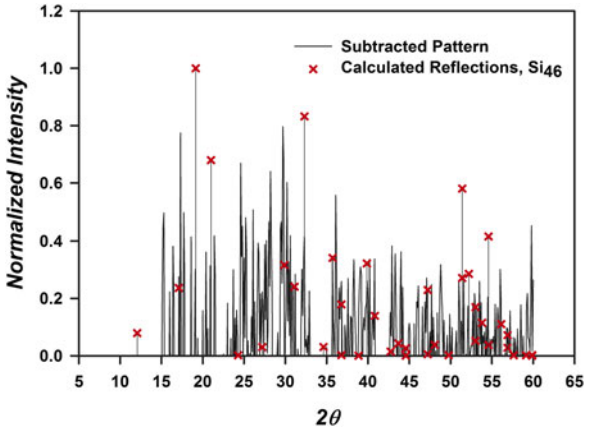

FIG. 1. Overlay of powder XRD patterns for the synthesized product and the calculated reflections of empty clathrate (Si_{46}), after subtraction of impurity phases.

III. RESULTS

A. Computational

Figure 2 presents the CPMD results of the energy of formation for crystalline Si (c-Si), amorphous Si (a-Si), crystalline $Li_{15}Si_4$ (c-$Li_{15}Si_4$), crystalline Si_{46} clathrate (c-Si_{46}), and three compositions of Type I crystalline lithium–silicon clathrates (c-Li_8Si_{46}, c-$Li_{24}Si_{46}$, and c-$Li_{48}Si_{46}$). The c-$Li_{15}Si_4$ compound has been shown to be the fully lithiated phase at room temperature for c-Si thin films.[36] The three clathrates are examples of lithium-silicon clathrates with moderate (166 mAh/g for Li_8Si_{46}) and high charge storage capacities (499 mAh/g for c-$Li_{24}Si_{46}$ and 999 mA h/g for $Li_{48}Si_{46}$). The energy of formation of c-Si at 0 K was computed to be −107.35 eV/Si atom at the equilibrium condition. This value was taken to be the reference, and the energy of formation for a-Si, Li_xSi_{46}, and $Li_{15}Si_4$ was computed

and presented relative to the energy of formation of c-Si. These results, presented in Fig. 2, show the energy change per Si atom as a function of the unit cell volume to the 1/3 power. The minimum in the energy curve gives the lattice parameter of the unit cell for a crystalline solid or the equivalent length scale for an amorphous solid. These results indicate that the energies of formation for a-Si and c-Si_{46} are comparable and both are higher than those of c-Si and c-$Li_{15}Si_4$, as shown in Fig. 2. The lattice parameter of c-Si (5.456 Å) is much smaller than that of c-$Li_{15}Si_4$ (10.642 Å). The equivalent lattice parameter of amorphous Si (a-Si), defined as a_o = (unit cell volume)$^{1/3}$, is about 5.533 Å and is also much smaller than that of $Li_{15}Si_4$ (10.642 Å). In contrast, the lattice parameter of Si_{46} (10.335 Å for experimental value[29] and 10.119 Å for the value computed here) matches well with that of c-$Li_{15}Si_4$ (10.642 Å).

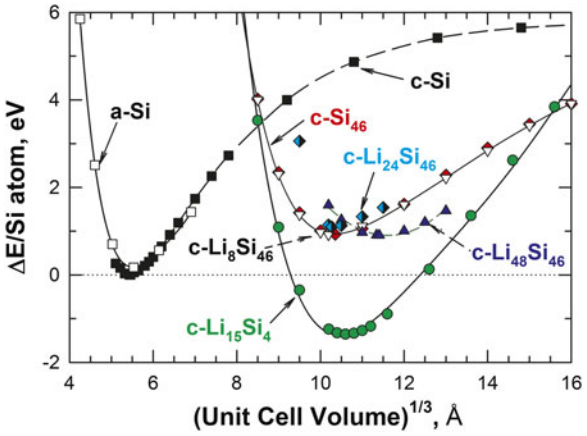

FIG. 2. Computed energy change per Si atom as a function of unit cell volume to the 1/3 power for c-Si, a-Si, c-Si_{46}, c-$Li_{15}Si_4$, c-Li_8Si_{46}, c-$Li_{24}Si_{46}$, and c-$Li_{48}Si_{46}$.

Calculations show that the lithiation of Si_{46} to form $Li_{15}Si_4$ would result in a volume expansion of only 9%, compared with 300% for the lithiation of crystalline Si to form $Li_{15}Si_4$.[2] This value of volume expansion (9%) corresponds to a lithiation strain of 3%, compared to 95% for crystalline Si. The lithiation strain is computed as the change in lattice constant of the anode before and after lithiation normalized by the initial lattice constant before lithiation. Lithiation of Si_{46} forms c-Li_8Si_{46} and $Li_{48}Si_{46}$, and results in lithiation strains of ≈0.77 and 10% and volume strains of ≈2.3 and 40% for Li_8Si_{46} and $Li_{48}Si_{46}$, respectively. The Si_{46}, Si_{20}, and Si_{24} cage structures are presented in Figs. 3(a), 3(b), and 3(c), respectively.

A systematic evaluation of the insertion of Li ions into a unit cell of c-Si_{46} indicates that the computed lattice constant, a_o, of Li_xSi_{46} clathrate remains relatively constant at 10.19 Å until the number of Li atoms inserted exceeds 24 (499 mAh/g), as shown in Fig. 4(a). The lattice constant of Li_xSi_{46} increases from 10.19 Å to 11.41 Å when the number of Li inserted, x, increases from 24 to 48. A further increase of Li ions beyond 48 (>999 mAh/g) causes the Type I cage structure to expand to a larger lattice constant. For comparison, Fig. 4(a) also shows the increases in the lattice constant for a-Si and c-Si as a function of Li to form a unit cell of lithium silicide ($Li_{15}Si_4$), which contains 60 Li atoms and 16 Si atoms. The corresponding energy change/Si values associated with the insertion of Li into silicon clathrate and a-Si are compared in Fig. 4(b). The value of the energy change/Si for insertion of Li into silicon clathrate is relatively constant at about 0.85–0.95 eV for up to 112 Li atoms. The positive energy change values indicate that the Li_xSi_{46} compounds are metastable and exhibit higher energy values

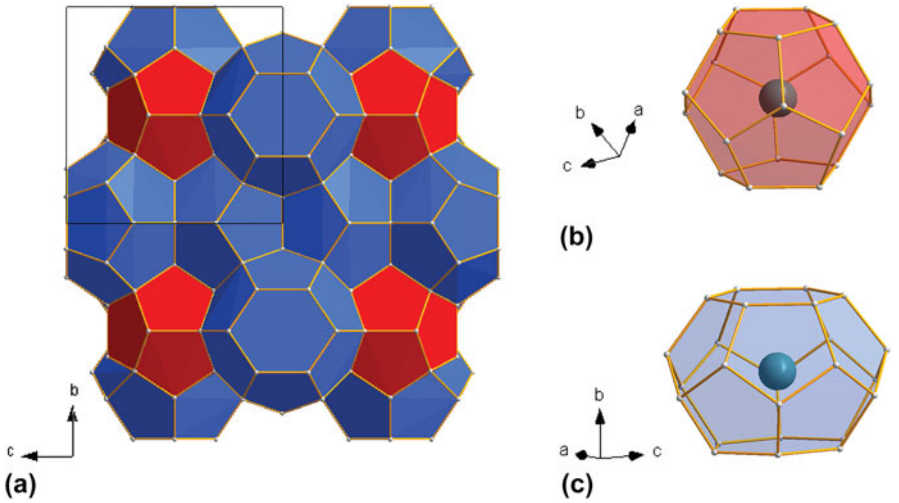

FIG. 3. The Si_{46}, Si_{20}, and Si_{24} cage structures for Type I silicon clathrate: (a) Si_{46} unit cell, (b) Si_{20} cage structure with a Li guest atom, and (c) Si_{24} cage structure with a Li guest atom.

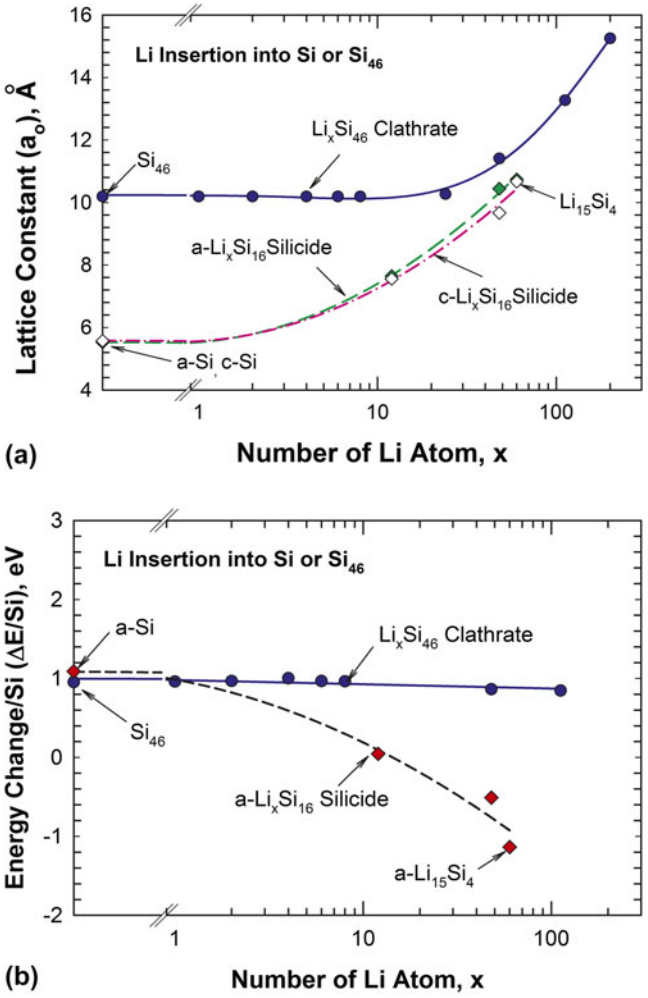

FIG. 4. Computed lattice constants of (a) Li_xSi_{46} clathrate and Li_xSi_{16} silicide, and (b) computed energy change/Si as a function number of Li atoms inserted.

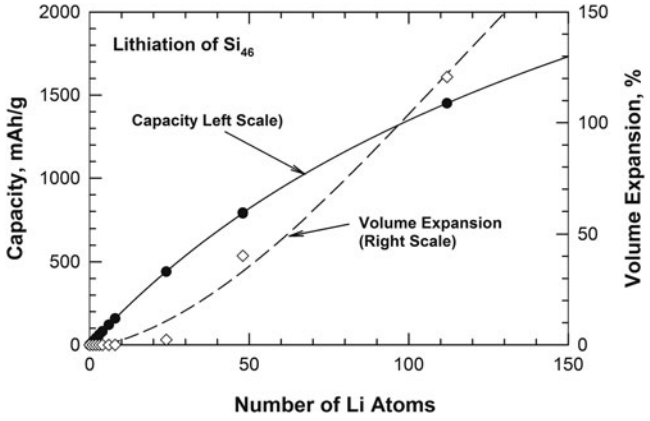

FIG. 5. Capacity and volume expansion as a function of number of Li atoms inserted into the cage structure of Si_{46}.

than either a-Si or $Li_{15}Si_4$. In contrast, the energy change/Si for Li insertion into a-Si to form $Li_{15}Si_4$ decreases with increasing number of Li atoms and reaches −1.136 eV at 60 Li atoms. These results indicate that there is a small energy barrier for the insertion of Li into the silicon clathrate and that the Li_xSi_{46} clathrate with $x < 112$ (2330 mAh/g) exhibits a higher energy than $Li_{15}Si_4$ silicide. Thus, there is a thermodynamic driving force for a possible phase transformation from Li_xSi_{46} to $Li_{15}Si_4$. A phase transformation from Li_xSi_{46} to $Li_{15}Si_4$ results in a relatively small change in the lattice constant, as shown in Fig. 4(a).

Figure 5 summarizes the results on the theoretical capacity of an empty Si_{46} as a function of Li atoms inserted into the cage structure and the corresponding volume expansion of the unit cell. Figure 5 shows that both capacity and volume expansion increases with lithiation, but at different rates. At lithiation levels of up to 24 Li atoms, the theoretical capacity increases with increasing Li atom insertion with little or no volume expansion (less than 2.3% volume strain). At 48 Li atoms, the theoretical capacity increases at a reduced rate to 791.6 mAh/g, while the volume expansion increases to 40.2% at increasing rates. At 112 Li atoms, the theoretical capacity reaches as high as 1450 mAh/g, while the volume expansion is about 120%.

B. Experimental results

Figure 6(a) shows the capacity based on the mass of the active material (left scale) and the coulombic efficiency (right scale) as a function of cycle number of the Si_{46} anode from 4 to 50 cycles. The first three cycles, which were in the SEI formation phase, are not presented in this figure. During the SEI formation, the capacity was 919 mAh/g at a 21% coulombic efficiency in the first cycle at a C rate of 0.21. The capacity decreased to 890 mAh/g at a 69% coulombic efficiency in the third cycle. The C rate was increased to 5.3 after the first three cycles. As shown in Fig. 6(a), the capacity of the Si_{46} anode was 675 mAh/g at 4th cycle, but increased to 809 mAh/g at 50 cycles at 5.3C. The corresponding coulombic efficiency was 99%. After a temporary pause at the 50th cycle and then restarting, the capacity jumped to 1030 mAh/g at the 51st cycle as shown in Fig. 6(b). Upon further cycling, the capacity dropped from 1030 to 553 mAh/g after 1000 cycles, as shown in Fig. 6(b).

Previous work by Li et al.[27] indicated that the dQ/dV response of Ba-stabilized Al-substituted clathrates is distinctly different from that associated with lithiation of crystalline Si or amorphous Si anodes. For comparison purposes, the dQ/dV response associated with the long-term cyclic tests of empty Si_{46} were obtained. The results for cycles 10, 100, 500, and 1000 are compared in Fig. 7. The breaks in the dQ/dV curves shown in Fig. 7 were caused by the fact that the data of the long-term cycling tests were acquired not continuously but at specified time intervals, which led to gaps in the acquired data during the transition from lithiation and delithiation, and vice

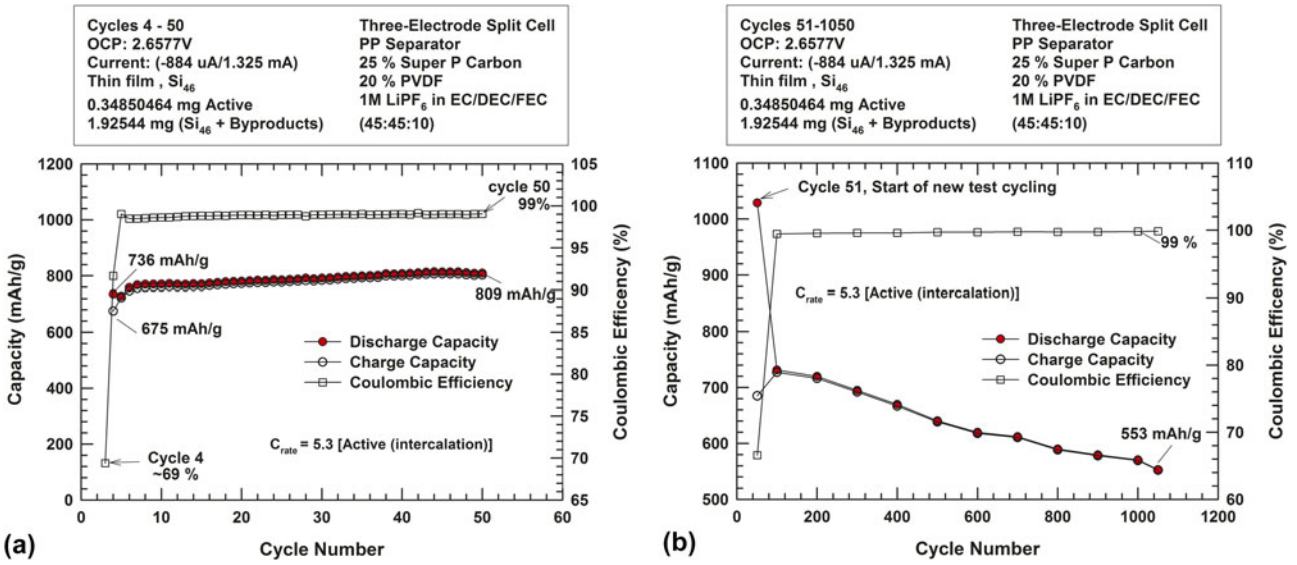

FIG. 6. Capacity and coulombic efficiency of a Si_{46} electrode during cycling (a) from the 4th to the 50th cycle, and (b) from the 51st to the 1050th cycle. The C rate was based on the mass of the active material.

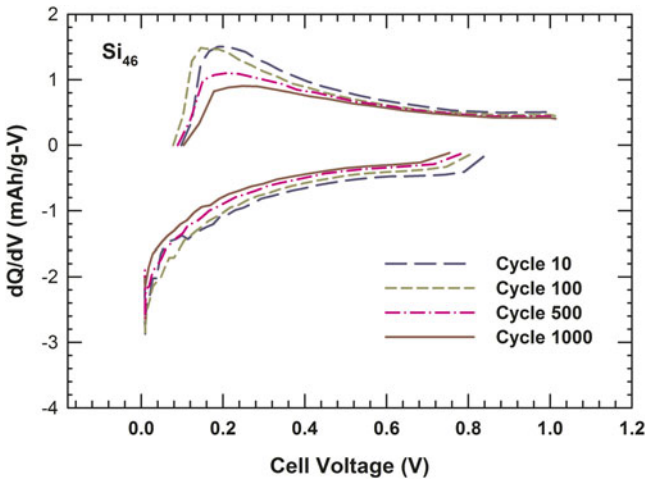

FIG. 7. Plot of dQ/dV as a function of cell voltage.

versa. The dQ/dV plots taken at various cycles are similar for empty Si_{46}, but the peak appears to shift to lower voltages as the cycle number increases.

IV. DISCUSSION

First-principles molecular dynamics computations indicate that the Li insertion process in silicon clathrate, which appears to be different from that of a-Si and c-Si, involves the storage of Li atoms in the open and accessible spaces within the cage structure of the clathrate. Recent work by Li et al.[27] showed the lithiation response of c-Si, amorphous Si, and Ba-stabilized Al-substituted silicon clathrates are indeed different with dQ/dV plots that exhibit different peaks at different voltages. Figure 8 shows a comparison of the dQ/dV plots of empty Si_{46} and $Ba_xAl_ySi_{46-y}$ clathrates. The comparison indicates that the dQ/dV peak for empty Si_{46} occurs at a lower voltage compared to those observed in $Ba_xAl_ySi_{46-y}$, even though the shape of the dQ/dV curves are similar. The shift in the peak location may be related to the ease of inserting or extracting Li atoms from the cage structure due to the presence of Ba guest atoms in the case of $Ba_xAl_ySi_{46-y}$ and its absence in the case of empty Si_{46}. To confirm the DFT results, we also computed the accessible volume of empty Si_{46} using the DMol^3 package in Materials Solution (Accelrys, UK) and a Li^+ probe (1.84 Å^3 volume). Theoretical computation revealed an accessible volume of 42.9 Å^3/unit cell for Si_{46}. This accessible volume of silicon clathrate can accommodate 23 Li ions, indicating adequate diffusion pathways for 23 Li ions. The insertion process can proceed without an enlargement of the clathrate structure until the open structure is filled with 24 Li atoms, which is in accordance with the CPMD results shown in Fig. 4(a). Figure 4(a) also shows that the lattice constant of the clathrate structure expands by about 12% upon insertion of 48 Li atoms. At this state, the energy change for Li_xSi_{46} is larger than those for a-Li_xSi_{46} and a-$Li_{15}Si_4$. Subsequent Li insertion can proceed via two paths: (i) expanding the clathrate structure to accommodate additional Li atoms, and (ii) transforming the Li_xSi_{46} clathrate structure to the Li_xSi_{16} (e.g., $Li_{15}Si_4$) silicide structure. A transformation to lithiated a-Si has been observed during lithiation of Type II Na-filled silicon clathrate (Na_xSi_{136}).[37,38]

The long-term cyclic tests suggest that Li atoms can be inserted and extracted from the cage cavities of Si_{46} clathrates. Previous studies[26–28] have also shown Li atoms can be inserted and extracted from the cage structure

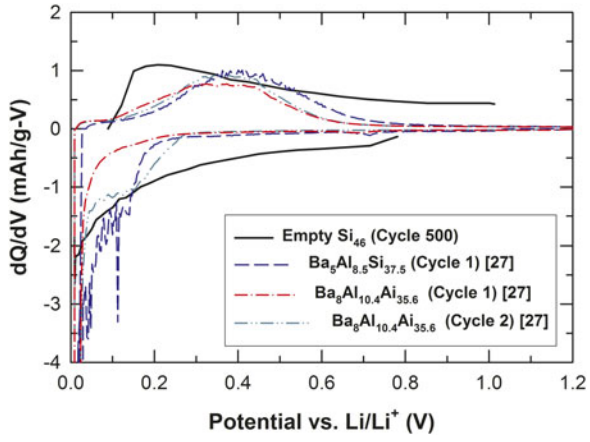

FIG. 8. A comparison of dQ/dV responses of Si_{46} and $Ba_xAl_ySi_{46-y}$ from the literature.[27]

of $Ba_xAl_ySi_{46-y}$ clathrates. However, the insertion and removal of Li atoms from the cage cavities of empty Si_{46} appears to be easier and leads to improved coulombic efficiency, higher capacity, and longer life compared to $Ba_8Al_8Si_{38}$. The observed capacities of empty Si_{46} were 675–809 mAh/g during stable cycling. The number of Li atoms required to achieve these observed capacities are computed to be 39 to 49, which are in agreement with theoretical predictions of a maximum of ≈48 Li based on density functional theory. At these capacity levels, Li atoms can be inserted and extracted in the presence of some volume changes (≈40% at Li = 48). A capacity increase was observed when the cell was held at open circuit between the 50th and 51st cycles during a pause. During this time, it is possible that there was an increase in the resistance of the SEI, which led to the large charge capacity of 1030 mAh/g but low coulombic efficiency of <70% observed in the 51st cycle. It is likely that the irreversible capacity was due to charge being used to re-form the SEI layer. The new SEI layer formed after the 50th cycle may have been thicker and more resistive, which may have impeded Li transport from the electrolyte to the clathrate.

After the 51st cycle, the discharge capacity started at ~700 mAh/g, a decrease from the 809 mAh/g observed in cycle 50. At the peak capacity (1030 mAh/g), the number of Li atoms inserted was computed to be 66 at which point the lithiated Si_{46} cage structure began to expand substantially (>120%), Fig. 5. The lower capacities observed after the 51st cycle may originate from overlithiation, which may have caused lattice expansion and possible damage to the clathrate cage structure or amorphization, or due to formation of a thick and resistive SEI layer after the open circuit period. The decrease in capacity from 1030 mAh/g at the 51st cycle to 553 mAh/g at the 1050th cycle corresponds to a reduction of the number of Li atoms inserted from 66 to 31. The corresponding volume of expansion associated with the cage structure also decreased from 120% at the peak capacity (51st cycle) to about 10% at the 1050th cycle when the long-term cyclic test was terminated. Despite a decrease in capacity, the Si_{46} electrode remained functional and the number of Li atoms into the cage exceeded those required to fill the accessible volume of an unexpanded cage. This finding indicates that the dimensions of the Si_{46} cage may be expandable and can be cycled in an expanded state over at least 1000 cycles. The decrease in capacity, however, suggests that Li_xSi_{46} may not be stable when $x > 48$ and overlithiation may lead to structural damages or amorphization of Si, depending on the lithiation path. Furthermore, the cage structure appears to be stable at low Li concentrations but may become unstable at high Li concentrations (e.g., >48 Li atoms).

In previous studies, the structural changes associated with unlithiated and lithiated Type I $Ba_8Al_8Si_{38}$ were studied using powder x-ray and neutron diffraction, x-ray photoelectron spectroscopy (XPS), and solid state nuclear magnetic resonance (NMR).[27,35] The diffraction techniques[27,35] did not reveal discernible changes in the clathrate crystal structure after lithiation and XPS confirmed the presence of an SEI layer after cycling.[27] ^{29}Si static NMR measurements of the lithiated clathrates showed spectra very similar to unlithiated clathrates.[27] In addition, magic angle spinning solid-state ^{27}Al NMR spectra indicated that Li insertion into the cage structure altered the relative amplitude of ^{27}Al NMR peaks at the 16i, 6c, and 24k sites, but no significant change in chemical shift or structural order was observed.[35] Similar characterization work was not performed on the unlithiated and lithiated Si_{46} because of limited resources. X-ray diffraction was performed on the lithiated Si_{46} but the results were not satisfactory due to the presence of strong Cu peaks from the collector. Attempts were also made to identify the extra peaks in the XRD pattern but without success. The extra peaks did not correspond to those of crystalline Si. Furthermore, none of the expected by-products, which included alkene, alkylamines, and Na_4Si_9, could be lithiated and should not have affected the lithiation response. On the other hand, some of the extra peaks could possibly be matched to the minor peaks of Type II Si_{34}, but major peaks of Si_{34} were missing. It is possible that the synthesized silicon clathrate products contained a mixture of Si_{46} and Si_{34} silicon clathrates.[37,38] Since previous studies have shown that the cycleability of Si_{34} is very limited[37,38] and can result in amorphization of Si, the presence of Si_{34} impurities in Si_{46} can adversely affect the long-term cyclic performance of Si_{46}. On this basis, the long-term cyclic performance of Si_{46} may be improved further by increasing the purity of the synthesized Si_{46} products. This could also enable the more detailed study of the structural changes after lithiation, as was previously undertaken for Type I $Ba_8Al_8Si_{38}$.

V. CONCLUSIONS

The conclusions reached in this investigation are as follows:

(1) Long-term cyclic tests performed on Si_{46} electrodes confirmed the prediction by first-principles computations that Li atoms can be inserted and stored within the empty cavities of the cage structure of Si_{46}.

(2) The theoretical studies show that Si_{46} structure is expandable and can accommodate Li atoms in excess of those required to completely fill the accessible volume of the empty Si_{46} cage.

(3) The empty Si_{46} can be cycled long-term for at least 1000 cycles in the expanded state with volume expansion ranging from 10% to 120%.

(4) Overlithiation of the Si_{46} electrodes beyond 66 Li atoms inserted per formula unit resulted in a decrease in capacities from 1030 mAh/g to 553 mAh/g.

ACKNOWLEDGMENTS

This work was supported by the Internal Research and Development Program (Project 18.R9890) of Southwest Research Institute® (SwRI®) and the Batteries for Advanced Transportation Technologies (BATT) Program at Lawrence Berkeley National Laboratory (LBNL) through Contract No. DEAC0205CH11231, with Dr. Michel Foure at LBNL as program manager. The contribution of C.K.C. was supported by the National Science Foundation through Grant No. DMR-1206795 and startup funds from the Fulton Schools of Engineering, Arizona State University (ASU). The first principles computations were performed at the Texas Advanced Computing Center of the TerraGrid network. The authors acknowledge the clerical assistance provided by Ms. Loretta Mesa, SwRI, in the preparation of the manuscript and Ms. Ran Zhao, Ph.D. student at ASU, in the preparation of Fig. 3.

REFERENCES

1. C.J. Wen and R.A. Huggins: Chemical diffusion in intermediate phases in the lithium–silicon system. *J. Solid State Chem.* **37**, 271 (1981).
2. A. Timmons and J.R. Dahn: Isotropic volume expansion of particles of amorphous metallic alloys in composite negative electrodes for Li-ion batteries. *J. Electrochem. Soc.* **154**, A444 (2007).
3. J. Graetz, C.C. Ahn, R. Yazami, and B. Fultz: Highly reversible lithium storage in nanostructured silicon. *Electrochem. Solid-State Lett.* **6**(9), A194 (2003).
4. T. Takamura, S. Ohara, M. Uehara, J. Suzuki, and K. Sekine: A vacuum deposited Si film having a Li extraction capacity over 2000 mA h/g with a long cycle life. *J. Power Sources* **129**, 96 (2004).
5. H. Kim, B. Han, J. Choo, and J. Cho: Three-dimensional porous silicon particles for use in high-performance lithium secondary batteries. *Angew. Chem., Int. Ed.* **47**, 1 (2008).
6. M. Green, E. Fielder, B. Scrosati, M. Wachtler, and J.S. Moreno: Structured silicon anodes for lithium battery applications. *Electrochem. Solid-State Lett.* **6**(5), A75 (2003).
7. C.K. Chan, H. Peng, G. Liu, K. McIlwrath, X.F. Zhang, R.A. Huggins, and Y. Cui: High performance lithium battery anodes using silicon nanowires. *Nat. Nanotechnol.* **3**, 31 (2008).
8. L-F. Cui, R. Ruffo, C.K. Chan, H. Peng, and Y. Cui: Crystalline–amorphous core–shell silicon nanowires for high capacity and high current battery electrodes. *Nano Lett.* **9**, 491 (2009).
9. R.B. Lewis, A. Timmons, R.E. Mar, and J.R. Dahn: In situ AFM measurements of the expansion and contraction of amorphous Sn–Co–C films reacting with lithium. *J. Electrochem. Soc.* **154**(3), A213 (2007).
10. A. Timmons and J.R. Dahn: In situ optical observations of particle motion in alloy negative electrodes for Li-ion batteries. *J. Electrochem. Soc.* **153**, A1206 (2006).
11. S.D. Beattie, D. Larcher, M. Morcrette, B. Simon, and J-M. Tarascon: Si electrodes for Li-ion batteries—A new way to look at an old problem. *J. Electrochem. Soc.* **155**(2), A158 (2008).
12. V.A. Sethuraman, M.J. Chon, M. Shimshak, V. Srinivasan, and P.R. Guduru: In situ measurements of stress evolution in silicon thin films during electrochemical lithiation and delithiation. *J. Power Sources* **195**, 5062 (2010).
13. J.Y. Eom, J.W. Park, H.S. Kwon, and S. Rajendran: Electrochemical insertion of lithium into multiwalled carbon nanotube/silicon composites produced by ballmilling. *J. Electrochem. Soc.* **153**(9), A1678 (2006).
14. Y. Zhang, X.G. Zhang, H.L. Zhang, Z.G. Zhao, F. Li, C. Liu, and H.M. Cheng: Composite anode material of silicon/graphite/carbon nanotubes for Li-ion batteries. *Electrochim. Acta* **51**, 4994 (2006).
15. Y. Zhang, Z.G. Zhao, X.G. Zhang, H.L. Zhang, F. Li, C. Liu, and H.M. Cheng: Pyrolytic carbon-coated silicon/carbon nanotube composites: Promising application for Li-ion batteries. *Int. J. Nanomanuf.* **2**(1/2), 4 (2008).
16. J.H. Ryu, J.W. Kim, Y-E. Sung, and S.M. Oh: Failure modes of silicon powder negative electrode in lithium secondary batteries. *Electrochem. Solid-State Lett.* **7**(10), A306 (2004).
17. R.A. Huggins and W.D. Nix: Decrepitation model for capacity loss during cycling of alloys in rechargeable electrochemical systems. *Ionics* **6**, 57 (2000).
18. H. Wu, G. Chan, J.W. Choi, I. Ryu, Y. Yao, M.T. McDowell, S.W. Lee, A. Jackson, Y. Yang, L. Hu, and Y. Cui: Stable cycling of double-walled silicon nanotube battery anodes through solid-electrolyte interphase control. *Nat. Nanotechnol.* **7**(5), 310 (2012).
19. H. Wu and Y. Cu: Designing nanostructured Si anodes for high energy lithium ion batteries. *Nano Today* **7**(5), 414 (2012).
20. M.K. Aydinol and G. Ceder: First-principles prediction of insertion potentials in Li–Mn for secondary Li batteries. *J. Electrochem. Soc.* **144**(11), 3832 (1997).
21. Y. Kubota, M.C.S. Escano, H. Nakanishi, and H. Kasai: Crystal and electronic structure of $Li_{15}Si_4$. *J. Appl. Phys.* **102**, 053704 (2007).
22. V.L. Chevrier, J.W. Zwanziger, and J.R. Dahn: First principles studies of silicon as a negative electrode materials for lithium-ion batteries. *Can. J. Phys.* **87**, 625 (2009).
23. V.L. Chevrier and J.R. Dahn: First principles model of amorphous silicon lithiation. *J. Electrochem. Soc.* **156**(6), A454 (2009).
24. V.L. Chevrier and J.R. Dahn: First principles studies of disordered lithiated silicon. *J. Electrochem. Soc.* **157**(4), A392 (2010).
25. Q. Zhang, W. Zhang, W. Wan, Y. Cui, and E. Wang: Lithium insertion in silicon nanowires: An ab initio study. *Nano Lett.* **10**, 3243 (2010).

26. K.S. Chan and M.A. Miller: Anodes—Synthesis and characterization of silicon clathrates for anode applications in lithium-ion batteries. *Energy Storage R&D*, FY2014 Final Report, Southwest Research Institute (2014).
27. Y. Li, R. Raghavan, N.A. Wagner, S.K. Davidowski, L. Baggetto, R. Zhao, Q. Cheng, J.L. Yarger, G.M. Veith, C. Ellis-Terrell, M.A. Miller, K.S. Chan, and C.K. Chan: Type I clathrates as novel silicon anodes: An electrochemical and structural investigation. *Adv. Sci.* **2**, 1500057 (2015). doi: 10.1002/advs.201500057.
28. X. Peng, Q. Wei, Y. Li, and C.K. Chan: First-principles study of lithiation of Type I Ba-doped silicon clathrates. *J. Phys. Chem. C* **119**(51), 28247 (2015). doi: 10.1021/acs.jpcc.5b07523.
29. G.B. Adams, M. O'Keeffe, A.A. Kemkov, O.F. Sankey, and Y-M. Huang: Wide-band-gap Si in open four-fold-coordinated clathrate structures. *Phys. Rev. B: Condens. Matter Mater. Phys.* **49**, 8084 (1994).
30. A. San-Miguel and P. Toulemonde: High-pressure properties of group IV clathrates. *High Pressure Res.* **25**, 159 (2005).
31. P. Mélinon, P. Kéghélian, A. Perez, B. Champagnon, Y. Guyot, L. Saviot, E. Reny, C. Cros, M. Pouchard, and A.J. Dianoux: Phonon density of states of silicon clathrates: Characteristic width narrowing effect with respect to the diamond phase. *Phys. Rev. B: Condens. Matter Mater. Phys.* **59**, 10099 (1999).
32. CPMD, Version 3.13, IBM Corp 1990-2008, MPI für Festkörperforschung Stuttgart, 1997–2001, http://www.cpmd.org.
33. R. Car and M. Parrinello: Unified approach for molecular dynamics and density functional theory. *Phys. Rev. Lett.* **55**(22), 2471 (1985).
34. A.M. Guloy, R. Ramlau, Z. Tang, W. Schnelle, M. Baitinger, and Y. Grin: A guest-free germanium clathrate. *Nature*, **443**, 320 (2006). doi: 10.1038/nature05145.
35. K.S. Chan, M.A. Miller, C. Ellis-Terrell, and C.K. Chan: Synthesis and characterization of empty silicon clathrates for anode applications in Li-ion batteries. In *Proceedings of 2016 MRS Spring Meeting*, March 28-April 1, 2016, Phoenix, AZ. MRS Advance, CJO 2016, doi: 10.1557/adv.2016.434.
36. J. Li and J.R. Dahn: An in-situ x-ray diffraction study of the reaction of Li with crystalline Si. *J. Electrochem. Soc.* **154**, A156 (2007).
37. T. Langer, S. Dupke, H. Trill, S. Passerini, H. Eckert, R. Pöttgen, and M. Winter: Electrochemical lithiation of silicon clathrate-II. *J. Electrochem. Soc.* **159**, A1318 (2012).
38. N.A. Wagner, R. Raghavan, R. Zhao, Q. Wei, X. Peng, and C.K. Chan: Electrochemical cycling of sodium-filled silicon clathrate. *ChemElectroChem*, **1**(2), 347 (2014).

CORRIGENDUM

First principles and experimental studies of empty Si_{46} as anode materials for Li-ion batteries – CORRIGENDUM

Kwai S. Chan, Michael A. Miller, Wuwei Liang, Carol Ellis-Terrell, and Candace K. Chan

doi: 10.1557/jmr.2016.408, Published by Materials Research Society with Cambridge University Press, 17 November 2016.

In Chan et al.[1], references 3–17 had several errors and mislabels. The following list is the corrected references:

3. L.Y. Beaulieu, T.D. Hatchard, A. Bonakdarpour, M.D. Fleischauer, and J.R. Dahn: Reaction of Li with alloy thin films studied by *in situ* AFM. *J. Electrochem. Soc.* **150**(11), A1457 (2003).

4. A. Timmons and J.R. Dahn: *In situ* optical observations of particle motion in alloy negative electrodes for Li-ion batteries. *J. Electrochem. Soc.* **153**, A1206 (2006).

5. S.D. Beattie, D. Larcher, M. Morcrette, B. Simon, and J.-M. Tarascon: Si electrodes for Li-ion batteries − A new way to look at an old problem. *J. Electrochem. Soc.* **155**(2), A158 (2008).

6. V.A. Sethuraman, M.J. Chon, M. Shimshak, V. Srinivasan, and P.R. Guduru: *In situ* measurements of stress evolution in silicon thin films during electrochemical lithiation and delithiation. *J. Power Sources* **195**, 5062 (2010).

7. J.Y. Eom, J.W. Park, H.S. Kwon, and S. Rajendran: Electrochemical insertion of lithium into multiwalled carbon nanotube/silicon composites produced by ballmilling. *J. Electrochem. Soc.* **153**(9), A1678 (2006).

8. Y. Zhang, X.G. Zhang, H.L. Zhang, Z.G. Zhao, F. Li, C. Liu, and H.M. Cheng: Composite anode material of silicon/graphite/carbon nanotubes for Li-ion batteries. *Electrochim. Acta* **51**, 4994 (2006).

9. Y. Zhang, Z.G. Zhao, X.G. Zhang, H.L. Zhang, F. Li, C. Liu, and H.M. Cheng: Pyrolytic carbon-coated silicon/carbon nanotube composites: promising application for Li-ion batteries. *Int. J. Nanomanuf.* **2**(1/2), 4 (2008).

10. J.H. Ryu, J.W. Kim, Y.-E. Sung, and S.M. Oh: Failure Modes of Silicon Powder Negative Electrode in Lithium Secondary Batteries. *Electrochem. Solid-State Lett.* **7**(10), A306 (2004).

11. R.A. Huggins and W.D. Nix: Decrepitation model for capacity loss during cycling of alloys in rechargeable electrochemical systems. *Ionics* **6**, 57 (2000).

12. J. Graetz, C.C. Ahn, R. Yazami, and B. Fultz: Highly reversible lithium storage in nanostructured silicon. *Electrochem. Solid-State Lett.* **6**(9), A194 (2003).

13. T. Takamura, S. Ohara, M. Uehara, J. Suzuki, and K. Sekine: A vacuum deposited Si film having a Li extraction capacity over 2000 mAh/g with a long cycle life. *J. Power Sources* **129**, 96 (2004).

14. H. Kim, B. Han, J. Choo, and J. Cho: Three-dimensional porous silicon particles for use in high-performance lithium secondary batteries. *Angew. Chem. Int. Ed.* **47**, 1 (2008).

15. M. Green, E. Fielder, B. Scrosati, M. Wachtler, and J.S. Moreno: Structured silicon anodes for lithium battery applications. *Electrochem. Solid-State Lett.* **6**(5), A75 (2003).

16. C.K. Chan, H. Peng, G. Liu, K. McIlwrath, X.F. Zhang, R.A. Huggins, and Y. Cui: High performance lithium battery anodes using silicon nanowires. *Nat. Nanotechnol.* **3**, 31 (2008).

17. L.-F. Cui, R. Ruffo, C.K. Chan, H. Peng, and Y. Cui: Crystalline-amorphous core-shell silicon nanowires for high capacity and high current battery electrodes. *Nano Lett* **9**, 491 (2009).

The authors regret these errors.

REFERENCE

1. K.S. Chan, M.A. Miller, W. Liang, C. Ellis-Terrell, and C.K. Chan: First principles and experimental studies of empty Si_{46} as anode materials for Li-ion batteries. *J Mater. Res.* **31**(23), 3657–3665 (2016). doi: 10.1557/jmr.2016.408.

DOI: 10.1557/jmr.2017.160

